NMR study of the T_1 relaxation dispersion in the smectic mesophase of 4-chlorophenyl 4-undecyloxybenzoate

E. Anoardo and D.J. Pusiol
Facultad de Matemática, Astronomía y Física, Universidad Nacional de Córdoba, Laprida 854, 5000 Córdoba, Argentina

C. Aguilera
Facultad de Ciencias Químicas, Universidad de Concepción, Casilla 3-C, Concepción, Chile
(Received 8 October 1993)

An experimental study of the Larmor frequency dependence of the proton spin-lattice relaxation time $[T_1(\nu_L)]$ was carried out in the range of $\nu_L = 7$ to 30 MHz. Two relaxation times describing the evolution of the longitudinal magnetization have been found to have different behaviors. One of them has been assigned to the relaxation of the protons belonging to the alkyl chain-$T_1^{\text{alkyl}}(\nu_L)$-. The $T_1^{\text{alkyl}}(\nu_L)$ dispersion behaves normally without signs of ^{1}H-^{35}Cl cross relaxation. The second one, called $T_{a\text{-}c}$, has a partial contribution from the protons bonded to the molecular core and those of the alkyl chain. Well defined ^{1}H-^{35}Cl quadrupole dips (QD) have been observed in the $T_{a\text{-}c}(\nu)$ dispersion curve, due to a cross-relaxation process between the core protons and the chlorine nucleus of the molecule. The shape of the dips are not symmetric, and cannot be fitted by Gaussian or Lorentzian functions. Computer simulations with asymmetric functions previously used in line shape analysis of incommensurate systems and organic glasses are discussed.

I. INTRODUCTION

The proton Larmor frequency dependence of nuclear magnetic spin-lattice relaxation time T_1 has been successfully used for the study of dynamical processes in liquid crystals and biological systems.[1–5] If the molecule contains quadrupole nuclei, an anomalous minimum appears in the $T_1(\nu)$ dispersion curve, as a result of an effective cross relaxation between the quadrupole nuclei and the protons. This phenomenon is called "quadrupole dip."[6–9]

The shape of the dips depends on the shape of the spectra of both I (protons) and S (quadrupole) systems, and on the involved relaxation processes. Using spin-temperature formalism, Kimmich *et al.*[1] have discussed the involved relaxation processes. In a undeuterated and non-quadrupole-nuclei-enriched system three energy reservoirs and consequently three spin temperatures (β_I, β_S, and the lattice one, β_0) are distinguished. Therefore, three relaxation paths are possible, with relaxation rates denoted by: (i) direct relaxation, (ii) cross coupling, and (iii) cross relaxation, respectively. By homo- and hetereonuclear dipole-dipole interactions *direct I relaxation* tends to equalize the proton spin and lattice temperatures. The *cross-coupling* relaxation mechanism takes into account the fact that the two involved spin-energy reservoirs are simultaneously influenced by two spin transitions, and so the $d\beta_I / dt$ rate also depends on β_S. If the spin I and the spin S resonances exactly overlap ($\nu_I = \nu_S$) the flip-flop transitions become spin-energy conserving (in an equivalent situation to the spin-like case) and therefore do not directly contribute to the spin-I–lattice relaxation.[1] Finally, the *cross-relaxation* mechanism describes the energy flow between the two spin-energy reservoirs via flip-flop transitions conserving the total spin energy. Such a mechanism is only relevant if the I and S resonance lines overlap, and consequently the shape of the dips is strongly determined by the shape of each resonance line.[10]

Multiexponential recovery of the I magnetization is therefore expected when the I levels nearly overlap the quadrupole S levels. However, three limiting cases leading a single exponential relaxation can be distinguished by introducing $T_{1,I,\text{eff}}$ and $T_{1,S,\text{eff}}$ as time constants which takes into account diverse rate contributions that are partially ineffective.

(1) $T_{1,S,\text{eff}} << T_{1,I,\text{eff}} << T_{1,\text{cr}}$: the spin temperature of quadrupole nuclei fastly keeps the lattice temperature. The effective proton relaxation is governed by the direct relaxation mechanism.

(2) $T_{1,S,\text{eff}} << T_{1,\text{cr}} << T_{1,I,\text{eff}}$: we have again $\beta_S \approx \beta_0$. The spin I reservoir relaxes indirectly via the spin S system by means of the cross-relaxation mechanism.

(3) $T_{1,\text{cr}} << T_{1,S,\text{eff}} << T_{1,I,\text{eff}}$: cross relaxation ensures the same temperature for both spin systems ($\beta_S \approx \beta_I$). In this case both I and S spins relax with the same rate by *all mechanisms simultaneously*, so that $T_{1,S,\text{eff}} \approx T_{1,I,\text{eff}}$.

The predominance on $T_{1,H,\text{eff}}$ of each relaxation mechanism strongly depends on the degree of level overlap. Therefore, it is reasonable to expect that close to the central frequencies of the dips the limiting cases (2) and (3) will only be relevant, while case (1) can dominate at the dip flanks.

The shape of the dips is related with the nuclear quadrupole resonance (NQR) absorption line. In particular, if spins I have a narrow resonance line and spins S a broad one, dip shapes are closely representative of the

NQR absorption line. Previous pure NQR studies carried on solids with different disorder degrees, such as organic glasses and incommensurate systems, revealed asymmetric line shapes.[11,12] This property was attributed to particular topological characteristics of these systems, which can be present in a different context in some liquid crystalline mesophases. In order to inquire about the symmetry of dip shapes in a liquid crystal, Larmor frequency steps had to be narrow enough. Due to the inadequate low frequency resolution of field-cycling techniques for nitrogen dip-shape analysis, we preferred to do it by conventional NMR T_1 measurements at higher frequencies. Of course, we needed a compound with quadrupole frequencies higher than those of ^{14}N. Therefore a liquid crystal with Cl incorporated in the core of the molecular body was synthesized.

II. EXPERIMENTAL DETAILS

A. Synthesis of 4-chlorophenyl 4-undecyloxybenzoate

68.1 g (0.5 mol) 4-hydroxymethylbenzoate in 200 ml of methylethylcetone were added to 25 g of K_2CO_3 and 137.7 g (0.55 mol) of ω-bromodecane. The mixture was refluxed for about 24 h. After the reaction period the separated solid was dissolved in ether and washed several times with a small amount of water. The solution was dried with $MgSO_4$ and recrystallized with ether. The yield was 138 g (86.2%) of 4-undeccyloxymethylbenzoate. In a second step, 120 ml of $KOH_{(ac)}$ were added to 0.34 mol 4-undecyloxymethylbenzoate. The solution was refluxed for 3 h with constant stirring; after this period the solution was concentrated to dryness. The solid was dissolved with enough water and the dried. The yield was 90 g (87.4%).

85 g (0.28 mol) 4-undecyloxybenzoic acid was mixed with 27 ml of thyonylchloride (SO_2Cl) and some drops of dimethylformamide. The mixture was refluxed for 5 hs. The rest of SO_2Cl was evaporated and the residual, distillate to 150°C and 1×10^{-3} mm Hg. The yield 60.5 g (66.5%).

23.9 g (0.21 mol) *p*-chlorophenol were dissolved in 200 ml of dry tetrahydrofurane (THF). After cooling the solution to 5°C, 26 ml of triethylamine (drop to drop) and 60.6 g of undecyloxybenzoic acid chloride were added to THF. The mixture was stirred at room temperature for 1 h. After this period the solution was refluxed for about 6 h. The solvent was concentrated with a rota-evaporator. The solid product was washed several times with cool water and dissolved in hot ethanol. A second recrystallization was carried out in methanol. The yield was 20.3 g (25.6%) of the final compound. Substances synthesized were checked by IR, ^1H NMR, differential thermal analysis (DTA), and elemental analysis.

Heating in the DTA apparatus, the sample melts at 66.3°C and the respective clearance point occurs at $T =$ 79.5°C. Cooling from the isotropic phase, the transition to the mesophase happens at $T = 73.9\,°C$ and the one to the crystalline phase at $T = 50\,°C$.

Figure 1 shows a diagram of the molecule. The chlorine atom is located at the end of one of the benzene rings forming the molecule core. Note that the position is similar to that of the nitrogen atom in cyanobiphenyls.[4]

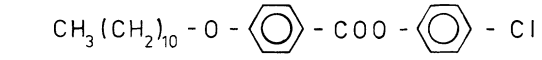

FIG. 1. Diagram of the 4-chlorophenyl 4-undecyloxybenzoate molecule. The chlorine atom is directly bounded to one of the two benzene rings.

B. $T_1(\nu_L)$ measurements

The Larmor frequency dependence of the longitudinal proton relaxation time, $T_1(\nu_L)$, was measured using a conventional, home-made and fully automatic NMR spectrometer. The apparatus is equipped with a Wavetek radio-frequency synthesizer model 2500, an Amplifier Research model 200L Transmitter, a Matec 625 receiver, and a Thurlby model DSA 524 data acquisition system. The temperature was measured by means of a cooper-Constantan thermocouple, and electronically controlled with a Eurotherm model 6250 system. An AT computer controls the whole measurements.

The material was sealed in glass tubes under vacuum by the usual freeze-thaw technique. With the purpose to orient the director field in a well-defined geometry relative to the Zeeman field, all relaxation measurements were preceded by heating the sample to the isotropic phase with the high magnetic field of the spectrometer on, and then cooled to the selected temperature in the smectic mesophase.

It was observed that the NMR free induction decay (FID) signal, has contributions from two different groups of protons, i.e., the alkyl chain and the core protons. Due to internal rotations of the CH_2 and CH_3 groups and the chain flexibility, it is expected that the alkyl chain protons will have larger mobility than those bounded to the core. That effect is experimentally reflected in the ^1H-NMR line widths; i.e., the chain-proton line is strongly narrowed. In the first attempt we use the conventional $\pi/2$-τ-$\pi/2$ technique. The integrated magnetization shows a nonexponential decay, due to the different T_1 of the above mentioned two protons groups. In a second step we use also conventional techniques involving deconvolution of the total NMR line in two peaks, but it was difficult to improve due to a low signal-to-noise ratio of the broad line. Nevertheless, the T_1 experiment at a given Larmor frequency, carried out by means of this technique, required about 30 min. The compound is easily decomposed by maintaining it in the mesophase for a few hours. For this reason it was necessary to implement, in the third step, the technique described by Fukushima and Roeder[13] and used in a similar experiment by Winter and Kimmich.[14] In this faster technique the sample is irradiated as usual by two $\pi/2$-τ-$\pi/2$ pulse sequences. The interval τ is measured when the ratio of the FID amplitudes following the first and second pulses respectively is $1/e$. This procedure has the advantage that in changing the Larmor frequency only the previous

τ had to be corrected. Due to the fact that the proton NMR signal has two different T_2^* decay constants, two spin-lattice relaxation times were measured in two different windows on the FID: one at the beginning of the signal, $T_{a\text{-}c}(\nu_L)$, where the two groups of protons make contributions, and the other at the end of the FID signal, $T_1^{\text{alkyl}}(\nu_L)$, where it is supposed that the chain protons are the only contributions present. In this way, $T_{a\text{-}c}$ represents relative variations between the two proton groups' spin-lattice relaxation times, while $T_1^{\text{alkyl}}(\nu_L)$ is directly associated with the longitudinal relaxation of the high mobility protons.

III. RESULTS

The relaxation study was carried out in the smectic mesophase at two temperatures: 65 and 75°C. Figures 2(a) and 2(b) show the $T_1^{\text{alkyl}}(\nu_L)$ and $T_{a\text{-}c}(\nu_L)$ behaviors for the lower and higher measured temperatures respectively. In both cases it is experimentally observed that $T_1^{\text{alkyl}}(\nu_L) > T_{a\text{-}c}(\nu_L)$. From a plateau at the lower Larmor frequencies, the $T_1^{\text{alkyl}}(\nu_L)$ smoothly increase with the frequency. At both temperatures, $T_1^{\text{alkyl}}(\nu_L)$ and $T_{a\text{-}c}(\nu_L)$ converge at low Larmor frequencies.

Dips in $T_{a\text{-}c}(\nu_L)$ are strongly observed at the two temperatures for frequencies higher than 20 MHz. While weak effects on the $T_{a\text{-}c}$ dispersion seem to be present between 10 and 20 MHz, as can be seen from the $T_1^{\text{alkyl}}(\nu_L)$ data, the protons of the alkyl chain do not relax via quadrupole dips in this frequency interval. It is important to note that the quadrupole dips, observed in $T_{a\text{-}c}(\nu_L)$, had to be necessarily associated with core protons. Consequently, only these protons relax via level crossing with the quadrupole chlorine nuclei. The center of the dips is shifted to lower frequencies as the temperature is increased. The effect is easily explained by assuming an effective dynamical averaging of the maximum electric field gradient (EFG) component at the ^{35}Cl nuclei. A strong temperature effect on the NQR spectrum as compared with those observed in solids has been previously reported for ^{1}H-^{14}N dips in liquid crystals. ^{37}Cl dips are barely observed at ν_L approximately 20 and 18 MHz at $T = 65$ and 75 °C, respectively (see Fig. 3).

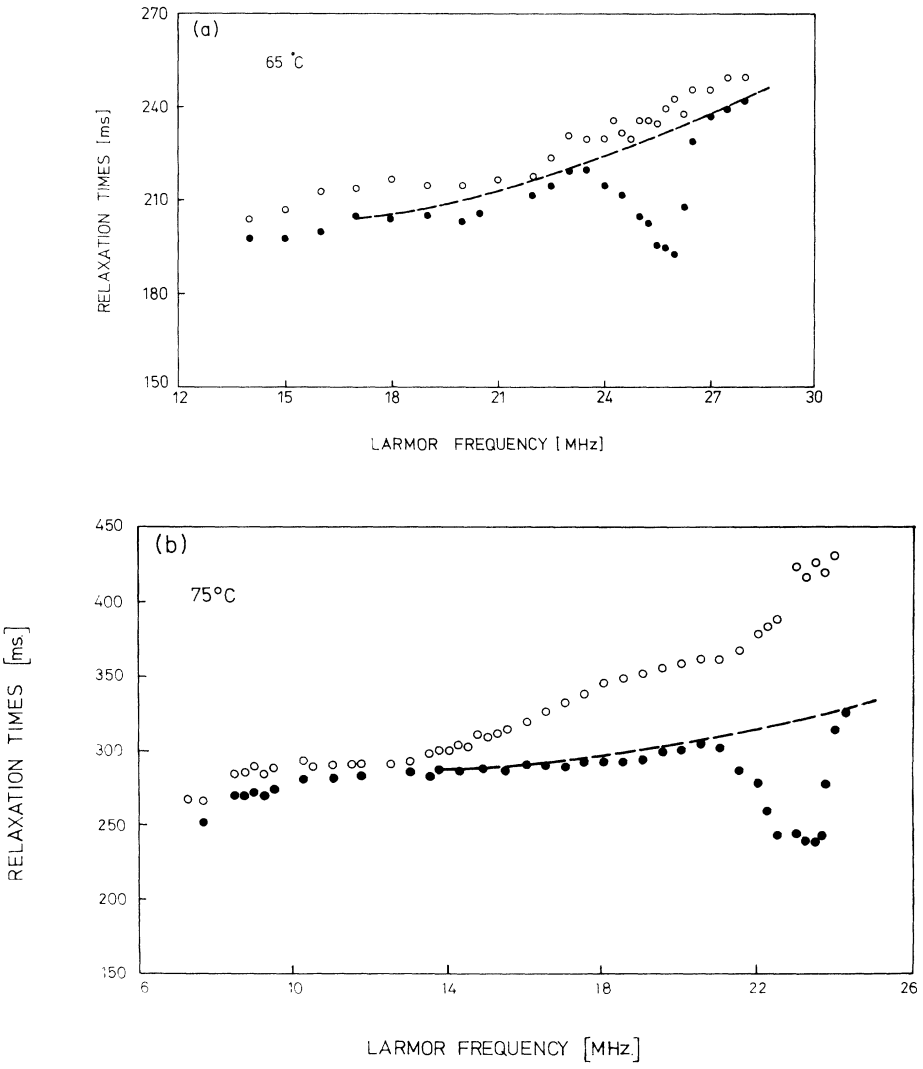

FIG. 2. (a) Experimental results of the spin-lattice relaxation times at $T = 65$ °C. Open circles represent the Larmor frequency behavior of T_1^{alkyl}. Quadrupole dips are clearly distinguished in the $T_1^{a\text{-}c}$ behavior (solid circles). The dotted line is the parabolic fitting of the $T_1^{\text{alkyl}}(\nu_L)$. The data points corresponding to the dip frequencies were arbitrarily removed. See Table I for the quadratic polynomial parameters. (b) The same as Fig. (a), but for $T = 75$ °C.

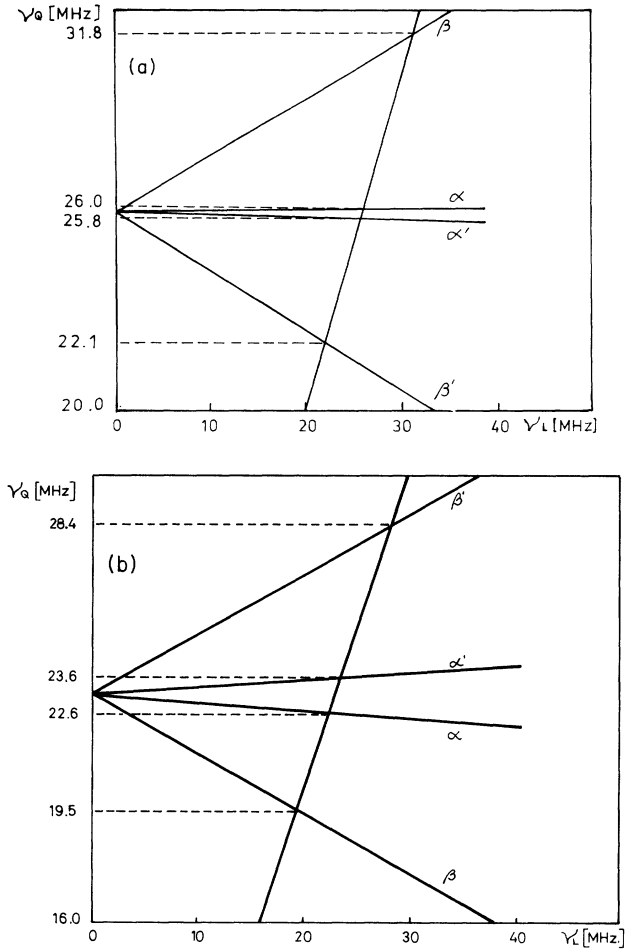

FIG. 3. Quadrupole and Zeeman crossing diagrams obtained by a compatibilization of the measured QD frequencies and tilt angles for the two experimental temperatures. (a) corresponds to $T = 65\ ^\circ\text{C}$ and $\theta = 56.2^\circ$. (b) is the same for $T = 75\ ^\circ\text{C}$ and the tilt angle is 46.6°. See Table II.

IV. DISCUSSION

A. Relaxation scheme

In order to analyze the quadrupole dips (QD's) quantitatively, one has to separate the relaxation dispersion due to proton-chlorine coupling from the effects due to proton-proton interactions.

The various possible relaxation mechanisms have been described elsewhere in the literature,[15–18] e.g., (i) internal rotations of a molecular group, R_i, rotational tumbling of the molecule about the long axis, $R_\parallel$, and about the short axis, $R_\perp$; (ii) orientational order fluctuation of the director OFD; and (iii) self-diffusion (SD) of the whole molecule. In the region away from critical effects the spin-lattice relaxation can be adequately expressed by the relative contribution of each mechanism. The relative contributions to the Larmor frequency dependence of the total relaxation rate, $1/T_1$, depend on the temperature and on the difference between their inverse correlation time.

Curve fitting to our experimental data, as is usually done in field cycling relaxation studies,[19] has no sense due to the narrow Larmor frequency interval in which measurements were carried out. In fact, all relaxation model functions vary slowly in this frequency interval, being possible to find several different fitting curves. In contrast, if the measured frequency interval covers six or seven magnitude orders, it is easier to identify the frequency intervals where different relaxation mechanisms dominate. Nevertheless, in order to analyze the dip shape in more detail, it is necessary to separate the proton-proton contribution to the relaxation dispersion curve in QD regions. Therefore, we decide to fit data without the experimental points corresponding to QD frequency intervals, by means of a polynomial function $T_{\text{HH}}(\nu_L)$ [see Figs. 2(a) and 2(b)], where $T_{\text{HH}}(\nu_L) = a + b\nu_L + c\nu_L^2$. Table I shows the parameters a, b and c corresponding to the two temperatures of the experiments.

$T_{\text{HH}}(\nu_L)$ represents the contribution from different proton-proton relaxation mechanisms to the total $T_{a\text{-}c}(\nu_L)$. We also define $T_{\text{HCl}}(\nu_L)$ as the contribution to $T_{a\text{-}c}(\nu_L)$ due to the protons and chlorine nuclei cross relaxation. These quantities are related by the relation

$$\frac{1}{T_{a\text{-}c(\nu_L)}} = \frac{1}{T_{\text{HH}}(\nu_L)} + \frac{1}{T_{\text{HCl}}(\nu_L)}, \tag{1}$$

from which is possible to obtain $1/T_{\text{HCl}}(\nu_L)$ with a good approximation. The $1/T_{\text{HCl}}(\nu_L)$ obtained are shown in Fig. 4.

B. Quadrupole dip analysis

1. *Frequency position of the dips*

In order to explain the number of expected dips appearing in $T_{a\text{-}c}(\nu_L)$, we should first analyze the $S = 3/2$ quadrupole nucleus Hamiltonian. Two part must be separated, i.e., (i) the pure quadrupole term and (ii) the Zeeman contribution. Owing to the fact that $\gamma_{\text{H}} \sim 10\gamma_{\text{Cl}}$, at the Larmor frequencies of the dips, the Zeeman energy of the chlorine is a tenth of the quadrupole one. Therefore, the Hamiltonian to be adopted must be the quadrupole plus a Zeeman perturbation term. If the asymmetry parameter is different from zero, a solution for $S = 3/2$ can be achieved.[20] The four frequencies corresponding to the possible transition are

$$\nu = \nu_Q \pm \frac{\gamma_{\text{Cl}} B_0}{4\pi}[f(m_1) \pm f(m_2)], \tag{2}$$

where

TABLE I. Fitting parameters of $T_{HH}(\nu_L)$ data by a parabolic formula. Data points measured at the dip frequency intervals were removed (see text).

T [°C]	a [ms]	b [10^{-9} s^2]	c [10^{-15} s^3]
65	245.9	- 6.50	0.20
75	340.2	- 9.20	0.36

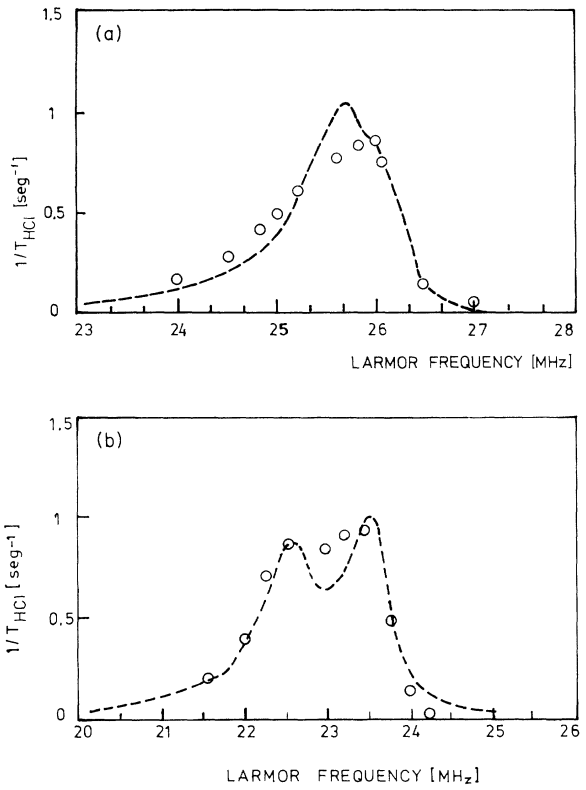

FIG. 4. Fitting of the strong QD using the formula of Eq. (17). A reasonable agreement is observed within the experimental dispersion.

$$\nu_Q = \frac{e^2qQ}{2\hbar}\left(1+\frac{\eta^2}{3}\right)^{1/2}, \tag{3}$$

$$f(m) = [a_m^2(\cos\theta)^2 + (b_m^2 + c_m^2 + 2b_m c_m \cos 2\phi)(\sin\theta)^2]^{1/2}, \tag{4}$$

$$\begin{aligned} a_{3/2} &= -1 - 2/\rho a_{1/2} = -1 + 2/\rho, \\ b_{3/2} &= 1 - 1/\rho b_{1/2} = 1 + 1/\rho, \\ c_{3/2} &= \eta/\rho = -c_{1/2}\rho = (1+\eta^2/3)^{1/2}, \end{aligned} \tag{5}$$

where θ, ϕ determine the relative orientation of the B_0 field in the principal axis system of the quadrupole Hamiltonian. The chlorine nucleus is bonded to the benzene ring in a way that the maximum electric field gradient component, q, is parallel to the long molecular axis. Within this geometry, rotation of the molecule along this axis minimizes η. For some compounds of the cyanobiphenyls and oxy-cyanobiphenyls series, η was previously measured.[4,25] The asymmetry parameter of the EFG at the nitrogen site—which is located at the same position in the molecule as the chlorine atom in 4-chlorophenyl 4-undecyloxybenzoate—was found to be smaller than 0.01. Moreover, the rf field was perpendicular to the external magnetic field, and therefore, the existence of an asymmetry parameter has a negligible influence.[21]

Assuming $\eta \approx 0$, the four Zeeman perturbed quadrupole spectrum can be reduced to the simplest expression

$$\begin{aligned} \nu_\alpha &= \nu_Q - [(3-\Delta)/2]\nu_L\cos\theta, \\ \nu'_\alpha &= \nu_Q + [(3-\Delta)/2]\nu_L\cos\theta, \\ \nu_\beta &= \nu_Q - [(3+\Delta)/2]\nu_L\cos\theta, \\ \nu'_\beta &= \nu_Q + [(3+\Delta)/2]\nu_L\cos\theta, \end{aligned} \tag{6}$$

where

$$\Delta = [1 + 4(\tan\theta)^2]^{1/2} \tag{7}$$

and

$$\nu_Q = \frac{e^2qQ}{2\hbar}. \tag{8}$$

θ is the angle between the Zeeman magnetic field and the electric field gradient. In spite of the fact that η could be very small, it can be supposed that the electric field gradient coincides with the longitudinal molecular axis. Therefore, if θ appears to be nonzero, a tilt angle in the smectic mesophase of the compound is expected. In the following, we describe the data analysis for both measured temperatures.

(i) 65 °C: In Fig. 2(a) it is easy to observe the appearance of a strong dip at approximately 26 MHz. The relation between the pure quadrupole frequencies for the two chlorine isotopes ^{35}Cl and ^{37}Cl due to their different quadrupole moments is 1:1.27. Taking into account this relation, ^{37}Cl dips must be centered at about 20.5 MHz. As can be seen in Fig. 2(a), a local minimum in the $T_{a\text{-}c}$ dispersion curve appears at approximately this frequency.

If the symmetry axis of the electric field gradient does not coincide with the direction of the magnetic field, there are four occurring frequencies [see Eqs. (6)], corresponding to the two $\alpha\alpha'$ and $\beta\beta'$ pairs. For the case of Zeeman splitting of quadrupole spectra with an axially symmetric field gradient, the inner pair $\alpha\alpha'$ has equal intensities.[22] The outer pair $\beta\beta'$ also has equal intensities, and the intensity ratio of the outer to inner pairs, I_β/I_α, is[22]

$$\frac{I_\beta}{I_\alpha} = \frac{\Delta-1}{\Delta+1}. \tag{9}$$

In the present case the $T_{a\text{-}c}(\nu_L)$ curve is weighted by $T_1^{\text{alkyl}}(\nu_L)$, and therefore, a little difference between the $\alpha\alpha'$ dip intensities is expected (this difference being greater the larger the frequency separation between the lines, and the stronger the $T_1^{\text{alkyl}}(\nu_L)$ variation in that frequency interval). A second smaller dip centered at about 22 MHz is present [Fig. 2(a)], which can be assigned to the β' line. Taking into account the fact that proton Larmor frequency is different in each dip position (ν_D), and that the relation $\nu_{Cl} \approx \nu_D/10$ holds, Eqs. (6) can be solved for θ and

$$\Delta\nu_\alpha = \nu_\alpha - \nu_{\alpha'}. \tag{10}$$

An approximate solution of θ was graphically obtained

[see Fig. 3(a)]. Once the value of θ is known, it follows from Eqs. (6) that

$$\Delta\nu_\alpha = \nu_Q\left[\frac{(\frac{3-\Delta}{10})\cos\theta}{(\frac{3-\Delta}{10})^2\cos^2\theta - 1}\right]. \quad (11)$$

Results are summarized in Fig. 3(a) and Table II.

As $\Delta > 3$ the pairs $\alpha\alpha'$ and $\beta\beta'$ are inverted. The intensity ratio calculated from (9) is about 0.5, but due to the cross-relaxation process between the dips and the pure splitted NQR lines, and that $T_{a\text{-}c}(\nu_L)$ is weighted by $T_1^{\text{alkyl}}(\nu_L)$, this parameter is not too significant.

(ii) 75 °C: A strong dip centered at about 23 MHz is found. According to this, the ^{37}Cl dip must be placed at approximately 18 MHz, where barely a minimum is observed in the $T_{a\text{-}c}(\nu_L)$ curve [Fig. 2(b)]. The β dip cannot be located from experimental data, but the separation of the α pair can be approximately obtained from a shape fitting of the dip (this point will be discussed in the next section). As can be seen, a separation of about 1 MHz is clearly distinguishable between the two minima observed in the strong dip. Solving (6) as before, it is possible to find the other dip positions and the angles. The results are summarized in Table II and Fig. 3(b).

2. *Shape of the dips*

Until now, the QD shape has been represented by Lorentzian or Gaussian functions.[1,4,25] Due to the strong asymmetry shown by the Cl dips in this compound, we had no success in fitting the data with Lorentzian or Gaussian functions. For example, in order to obtain a good least-squares fit of the dips, two Gaussian functions with different widths are necessary for the $\alpha\alpha'$ pair. The coexistence of this functions has no physical significance. Therefore, we found it convenient to do it by means of asymmetric line-shape functions used successfully in a previous NQR line-shape study of glassy and crystalline states of chlorobenzene solution in pyridine.[12]

The nuclear quadrupole frequency is proportional to the maximum component of the electric field gradient (q) at the observed quadrupole nucleus site (chlorine in the present case). Two kinds of contributions to q are present: *intra- and intermolecular ones.* Both contributions are summed ($q = q_{\text{intra}} + q_{\text{inter}}$). It is commonly accepted that q_{intra} is independent of the molecular surrounding. In contrast, the intermolecular contribution depends on the particular arrangement of neighboring molecules. Therefore, q_{inter} is dispersed by the relative positions and orientations of the nearest molecule. One can expect the general quadrupole spectrum of a liquid crystal, built up by overlapping the individual spectral lines of each molecules. The spectrum is then broadened—with respect to that of the crystalline solid—by the effect of the characteristic local deformations in liquid crystals. The resultant line shape will be symmetric or asymmetric depending on the statistical distribution law of the local deformations.

The density of the spectral line $\rho(\nu)$ and the statistical distribution of the electric field gradients $f(u)$ can be related as $\rho(\nu)d\nu = f(u)du$, where u represents an intermolecular spacing and orientational field. The resonant frequency at a given position can be expanded in powers of u:

$$\nu = \nu_0 + a_1u + 1/2a_2u^2 + \cdots . \quad (12)$$

Assuming

$$f(u) = \exp\left(-\frac{u^2}{2\sigma^2}\right), \quad (13)$$

with σ the Gaussian half-width, and a Lorentzian line shape for a given site,

$$L(\nu - \nu_c) = \frac{a}{1 + b(\nu - \nu_c)^2}, \quad (14)$$

the composed spectrum will be given by

$$F(\nu) = \int_{-\infty}^{\infty} L(\nu - \nu_0)\rho(\nu_c)d\nu_c. \quad (15)$$

If both linear and quadratic terms in the expansion of ν in powers of u are taken into account, a expression for $\rho(\nu)$ is obtained for two limiting cases: $a_2 > 0$ or $a_2 < 0$.[12] Keeping the $a_2 < 0$ solution (in accord with the type of asymmetry), after a little calculation, the final expression of $F(\nu)$ for dip-shape fitting is

$$F(\nu) = F_+(\nu) + F_-(\nu), \quad (16)$$

where

$$F_\pm(\nu) = aa_2\int_\infty^0 \frac{\exp[-\frac{(\chi\pm\xi)^2}{2\sigma^2}]}{1 + b[\nu - \nu_0 - a_2(\xi^2 - \chi^2)]^2}d\xi, \quad (17)$$

$$\xi = \sqrt{\chi^2 + \frac{2}{a_2}(\nu - \nu_0)}, \quad (18)$$

$$\chi = \frac{a_1}{a_2}, \quad (19)$$

where ν_0 is the frequency corresponding to the maximum

TABLE II. Predicted Zeeman perturbed quadrupole spectrum at the two measured temperature. The molecular tilt angle θ is compatible with the measured QD frequencies.

T [°C]	θ [deg]	$\nu_{\beta'}$ [MHz]	$\nu_{\alpha'}$ [MHz]	ν_α [MHz]	ν_β [MHz]
65	56.2	22.1	25.8	26.0	31.8
75	46.6	28.4	23.6	22.6	19.5

TABLE III. Parameters used to simulate the shape of the QD at the two measured temperatures evaluating equation (17). Figure 4 shows the data points and simulated behavior matching.

T [°C]	$\nu_{0\alpha}$ [MHz]	$\nu_{0\alpha'}$ [MHz]	a [10^6 s^{-2}]	b 10^{-3} [MHz^{-2}]
65	26.0	25.8	1.5	3.3
75	22.6	23.6	2.5	2.0

χ [MHz]	a_2 [MHz^{-1}]	σ [MHz]	$I_\alpha/I_{\alpha'}$
0.1	-0.12	0.29	1.007
0.1	-0.08	0.32	0.68

of the line. Figure 4 shows data and a computer simulation of the $\alpha\alpha'$ pair for both measured temperatures. Parameters involved in the simulated $1/T_{\mathrm{HCl}}$ are summarized in Table III.

Results obtained using asymmetric functions are shown to be better than those intended with Gaussian or Lorentzian functions. The asymmetry observed in both cases is similar.

3. *Implications of* $\theta \neq 0$

At both temperatures, the maximum electric field gradient directions at the ^{35}Cl nuclei and the external Zeeman field are nonparallel ($\theta \neq 0$). In the present analysis, the electric field gradients at the chlorine nuclei positions are assumed to have cylindric symmetry around the longitudinal molecular axis ($\eta \approx 0$). Therefore, the longitudinal molecular axis and the direction of the external magnetic field are nonparallel too. This fact tells us that the molecules are not aligned with the magnetic field. Additionally, due to the fact that the experimental NMR signal corresponds to the one characteristic of smectic mesophases, we assume that 4-chlorophenyl 4-undecyloxybenzoate has a tilted smectic C liquid crystalline structure.

From the above analysis of the $\alpha\alpha'$ and $\beta\beta'$ dip frequency positions, it is observed that the tilt angle diminishes as the temperature increases ($\theta_{65\,^\circ\mathrm{C}} > \theta_{75\,^\circ\mathrm{C}}$). This effect is compatible with previous observations in TBBA[23,24] for instance.

V. CONCLUDING REMARKS

The existence of quadrupole dips on the T_1 dispersion, using a conventional NMR apparatus, has been demonstrated. The experiment would confirm quadrupole dips previously found in other thermotropic liquid crystals with similar molecular structure—cyano- and oxycyanobiphenyls—by using the fast field cycling NMR technique.[4,25]

The existence of two distinguishable relaxation times is explained assuming the chlorine nuclei strongly coupled to the molecular core protons, which are of course the nearest neighbors. Perhaps, an additional decoupling between the chlorine and the alkyl chain protons could be the fast motions having the last ones.

The asymmetric shape of the dips has been explained assuming a local distortion field of molecular displacement and orientations, which disperse the electric field gradient component at the chlorine nucleus sites. A deeper analysis of the physical significance of local disorder on the quadrupole line shape in liquid crystals is actually being developed by our group. The corresponding results will be published elsewhere.

ACKNOWLEDGMENTS

The NMR spectrometer setup and the experimental measurements were carried out with the collaboration of Dr. A. Wolfenson. This research was partially financed by Fundación Antorchas, CONICOR and CONICET of Argentina.

[1] R. Kimmich, F. Winter, W. Nusser, and K.-H. Spohn, J. Magn. Reson. **68**, 263 (1986).
[2] E. Rommel, F. Noack, P. Meier, and G. Kothe, J. Phys. Chem. **92**, 2981 (1988).
[3] F. Noack, M. Notter, and W. Weiss, Liq. Cryst. **3**, 907 (1988).
[4] D. Pusiol and F. Noack, Liq. Cryst. **5**, 377 (1989).
[5] W. Nusser and R. Kimmich, J. Phys. Chem. **94**, 5637 (1990).
[6] D. Woessner and H. Gutowsky, J. Chem. Phys. **29**, 804 (1958).
[7] G. Voigt and R. Kimmich, J. Magn. Reson. **24**, 149 (1976).
[8] H. Stokers, T. Case, D. Ailion, and C. Wang, J. Chem. Phys. **70**, 3563 (1979).
[9] P. O. Westlund and H. Wennerstrom, J. Magn. Reson. **63**, 280 (1985).
[10] A. Abragam, *The Principles of Nuclear Magnetism* (Clarendon Press, Oxford, 1962).
[11] A. Wolfenson, D. Pusiol, and A. Brunetti, Z. Naturforsch A **45**, 334 (1990).
[12] A. Wolfenson, A. Brunetti, D. Pusiol, and W. Pontushka, Phys. Rev. B **41**, 6257 (1990).
[13] E. Fukushima and S. Roeder, *Experimental Pulse NMR* (Addison-Wesley, London, 1981).
[14] F. Winter and R. Kimmich, Biochim. Biophys. Acta **719**, 292 (1982).
[15] R. Blinc, M. Luzar, M. Vilfan, and M. Burgar, J. Chem. Phys. **63**, 3445 (1975).
[16] H. Pfeiffer, Ann. Phys. (N.Y.) **7**, 1 (1961).
[17] M. Vilfan and S. Zumer, Phys. Rev. A **21**, 172 (1980).

[18]D. Woessner, J. Chem. Phys. **37**, 647 (1962).
[19]F. Noack, Prog. Nucl. Magn. Reson. Spectrosc. **18**, 171 (1986).
[20]C. Dean, Phys. Rev. **96**, 1053 (1954).
[21]R. Creel, S. Segel, and A. Anderson, J. Chem. Phys. **50**, 4908 (1969).
[22]T. Das and L. Hahn, *Nuclear Quadrupole Resonance Spectroscopy* (Academic Press, New York, 1958).
[23]P. de Gennes, *The Physics of Liquid Crystals* (Clarendon Press, Oxford, 1974).
[24]G. Vertogen and W. de Jeu, *Thermotropic Liquid Crystals, Fundamentals* (Springer-Verlag, Berlin, 1988).
[25]D. Pusiol, R. Humpfer, and F. Noack, Z. Naturforsch A **47**, 1105 (1992).